



# HHS Public Access

Author manuscript

*Angew Chem Int Ed Engl.* Author manuscript; available in PMC 2018 February 01.

Published in final edited form as:

*Angew Chem Int Ed Engl.* 2017 February 01; 56(6): 1525–1529. doi:10.1002/anie.201610888.

## Enhancing the Cell Permeability and Metabolic Stability of Peptidyl Drugs by Reversible Bicyclization

**Dr. Ziqing Qian,**

Department of Chemistry and Biochemistry, The Ohio State University, 484 West 12th Avenue, Columbus, OH 43210 (USA)

**Curran A. Rhodes,**

Department of Chemistry and Biochemistry, The Ohio State University, 484 West 12th Avenue, Columbus, OH 43210 (USA)

**Lucas C. McCroskey,**

Department of Chemistry and Biochemistry, The Ohio State University, 484 West 12th Avenue, Columbus, OH 43210 (USA)

**Jin Wen,**

Department of Chemistry and Biochemistry, The Ohio State University, 484 West 12th Avenue, Columbus, OH 43210 (USA)

**George Appiah-Kubi,**

Department of Chemistry and Biochemistry, The Ohio State University, 484 West 12th Avenue, Columbus, OH 43210 (USA)

**Dr. David J. Wang,**

Department of Molecular Virology, Immunology, and Medical, Genetics, The Ohio State University, Columbus, OH 43210 (USA)

**Prof. Dr. Denis C. Guttridge,** and

Department of Molecular Virology, Immunology, and Medical, Genetics, The Ohio State University, Columbus, OH 43210 (USA)

**Prof. Dr. Dehua Pei**

Department of Chemistry and Biochemistry, The Ohio State University, 484 West 12th Avenue, Columbus, OH 43210 (USA)

### Abstract

Therapeutic applications of peptides are currently limited by their proteolytic instability and impermeability to the cell membrane. Here, we report a general, reversible bicyclization strategy to increase both the proteolytic stability and cell permeability of peptidyl drugs. A peptide drug is fused with a short cell-penetrating motif and converted into a conformationally constrained bicyclic structure through the formation of a pair of disulfide bonds. The resulting bicyclic peptide has greatly enhanced proteolytic stability as well as cell-permeability. Once inside the cell, the disulfide bonds are reduced to produce a linear, biologically active peptide. This strategy was

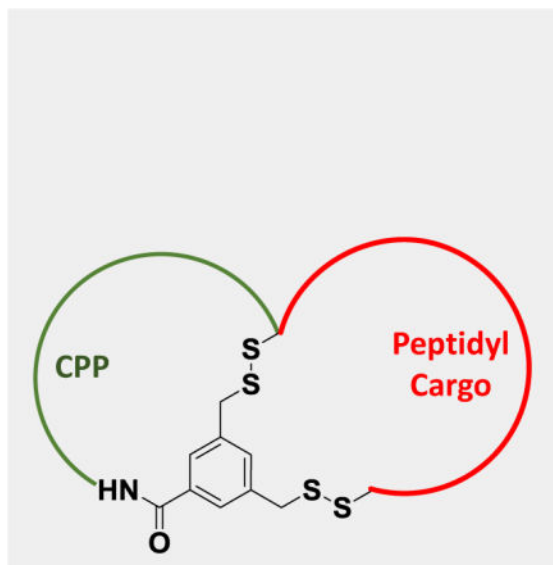
---

Supporting information for this article is given via a link at the end of the document

applied to generate a cell-permeable bicyclic peptidyl inhibitor against the NEMO-IKK interaction.

## Drug delivery

Peptide bicyclization via a pair of disulphide bonds increases its proteolytic stability and cell permeability and yet allows for regeneration of the functional linear peptide once inside the cytosol of the cell.



## Keywords

Cell-penetrating peptide; cyclic peptide; NEMO inhibitor; bicyclization; protein-protein interaction

Compared to small-molecule drugs, peptides are highly selective and efficacious and, at the same time, relatively safe and well tolerated. A particularly exciting application of peptides is the inhibition of protein-protein interactions (PPIs), which remain challenging targets for small molecules.<sup>[1]</sup> Consequently, there is an increased interest in peptides in pharmaceutical research and development, and ~140 peptide therapeutics are currently being evaluated in clinical trials.<sup>[2]</sup> However, peptides are inherently susceptible to proteolytic degradation. Additionally, peptides are generally impermeable to the cell membrane, largely limiting their applications to extracellular targets. Although N-methylation of the peptide backbone and formation of intramolecular hydrogen bonds have been shown to improve the proteolytic stability and membrane permeability of certain cyclic peptides,<sup>[3,4]</sup> alternative strategies to increase both the metabolic stability and cell permeability of peptide drugs are clearly needed.

NF- $\kappa$ B is a transcription factor that controls the expression of numerous gene products involved in immune, stress, inflammatory responses, cell proliferation, and apoptosis.<sup>[5]</sup> Aberrant activation of NF- $\kappa$ B signaling has been implicated in a number of autoimmune

diseases (e.g., rheumatoid arthritis) and cancer (e.g., diffuse large B-cell lymphoma), among others.<sup>[6]</sup> Canonical NF- $\kappa$ B signaling is mediated by the interaction between the inhibitor of  $\kappa$ B (I $\kappa$ B)-kinase (IKK) complex and regulatory protein NF- $\kappa$ B essential modifier (NEMO).<sup>[7]</sup> Binding to NEMO activates IKK, which in turn phosphorylates I $\kappa$ B, promoting the proteasomal degradation of I $\kappa$ B and release of active NF- $\kappa$ B. Modulators targeting various steps of the NF- $\kappa$ B signaling pathway have been reported, and some of them have progressed into the clinic.<sup>[6,8]</sup> One attractive strategy for ameliorating the NF- $\kappa$ B activity is to selectively disrupt the IKK-NEMO interaction. Previous studies generated a weak NEMO inhibitor ( $K_D \sim 37 \mu\text{M}$ ), Antp-NBD (Table 1, peptide **1**), which consists of the 11-residue NEMO-binding domain (NBD) of IKK $\beta$  covalently linked to a cell-penetrating peptide (CPP), Antp.<sup>[9]</sup> Interestingly, Antp-NBD blocks the IKK activity stimulated by different pro-inflammatory stimuli, but does not affect the basal NF- $\kappa$ B activity, thus providing a potentially safe and effective mechanism for reducing aberrant NF- $\kappa$ B activity.<sup>[9]</sup> In several pre-clinical studies, Antp-NBD demonstrated *in vivo* efficacy for treating Duchenne muscular dystrophy and large B-cell lymphoma in mouse and canine models.<sup>[10]</sup> However, to achieve clinical utility, Antp-NBD would benefit significantly from improvements in its NEMO-binding affinity, metabolic stability, and cell-permeability.

We previously reported cyclo(F $\Phi$ RRRRQ) (cF $\Phi$ R<sub>4</sub>, where  $\Phi$  is L-2-naphthylalanine) as a member of a novel class of cyclic CPPs.<sup>[11]</sup> These CPPs bind directly to the membrane phospholipids, enter cells by endocytosis, and efficiently escape from the early endosome into the cytosol by inducing budding of small, unstable vesicles.<sup>[11,12]</sup> With a cytosolic delivery efficiency (defined as the ratio of cytosolic over extracellular cargo concentration) of 20%, cF $\Phi$ R<sub>4</sub> is an order of magnitude more active than Tat, one of the most widely used CPPs.<sup>[12]</sup> Most importantly, cF $\Phi$ R<sub>4</sub> and other cyclic CPPs are capable of efficiently delivering a variety of cargo molecules including small molecules, peptides, and proteins into the cytosol of mammalian cells.<sup>[11]</sup> For example, short peptidyl cargos were directly incorporated into the cF $\Phi$ R<sub>4</sub> ring (endocyclic delivery) and the resulting cyclic peptides were cell-permeable.<sup>[11–13]</sup> cF $\Phi$ R<sub>4</sub> was also fused with 5.7 million different cyclic peptides to generate a library of cell-permeable bicyclic peptides (bicyclic delivery).<sup>[14]</sup> However, many peptide ligands must be in their extended conformations to be biologically active and are not compatible with the above cyclization approaches. To this end, we recently developed a reversible cyclization strategy for intracellular delivery of linear peptidyl ligands, by fusing them with F $\Phi$ R<sub>4</sub> and cyclizing the fusion peptides through a disulfide bond.<sup>[15]</sup> Unfortunately, the previous approach is limited to relatively short peptides, as cyclization of longer peptides results in large rings, whose conformational flexibility limits the gains in metabolic stability and cell-permeability.<sup>[11]</sup> Cyclization via an internal cysteine results in smaller rings and better cellular uptake, but leaves a portion of the peptidyl cargo in the linear form, which remains susceptible to proteolytic degradation. To overcome this limitation, we report here a reversible bicyclization strategy, which allows the entire CPP-cargo fusion to be converted into a bicyclic structure by the formation of a pair of disulfide bonds (Scheme 1). When outside the cell, the peptide exists as a highly constrained bicycle, which possesses enhanced cell permeability and proteolytic stability. Upon entering the cytosol, the disulfide bonds are reduced by the intracellular glutathione (GSH) to produce the linear, biologically active peptide. The bicyclic system permits the formation of a small

CPP ring for optimal cellular uptake<sup>[11]</sup> and a separate cargo ring to accommodate peptides of different lengths.

To test the validity of the reversible bicyclization strategy, we first designed two model peptides consisting of the CPP motif (RRRRΦF or FΦRRRR) and a mock cargo motif (SASAS) fused to its N- or C-terminus (Table 1, peptides **2** and **3**, Figure S1 for detailed structures). Two cysteine residues were also incorporated into the sequences for later cyclization, one at the junction between the CPP and cargo motifs and one at the C-terminus. The linear peptides were synthesized by standard Fmoc solid-phase peptide synthesis (SPPS) chemistry on Rink amide resin (Scheme 2). The acetamidomethyl (Acm) groups on the two cysteine side chains were selectively removed by treatment with Hg(OAc)<sub>2</sub> and the exposed free thiols were then reacted on-resin with 3,5-bis((pyridin-2-yl)disulfanyl)methyl)benzoic acid, which was readily prepared from commercially available starting materials (Scheme S1). Formation of two disulfide bonds between the cysteine side chains and the 3,5-bis(mercaptomethyl)benzoic acid (BMB) scaffold resulted in cyclization of the peptide. Next, the N-terminal Fmoc group was removed by 1,8-diazabicyclo[5.4.0]undec-7-ene (DBU) and the peptide was bicyclized by forming a lactam between the carboxyl group of BMB and the N-terminal amine (Scheme 2). BMB is ideally suited as the scaffold, because its structural symmetry ensures that a single bicyclic product is formed following the disulfide exchange reactions. Additionally, the rigidity of the scaffold prevents the formation of any intramolecular disulfide bond, simplifying both the synthesis of the scaffold and its reaction with the cysteine-containing peptides.

To monitor their cellular uptake, peptides **2** and **3** were labeled with fluorescein isothiocyanate (FITC) on the side chain of a C-terminal lysine. Flow cytometry analysis of HeLa cells treated with 5 μM peptides cFΦR<sub>4</sub>, **2** and **3** for 2 h showed mean fluorescence intensity (MFI) values of 3020, 5180, and 4100, respectively (Figure 1a). Thus, bicyclic peptides **2** and **3** entered HeLa cells with 72% and 36% higher efficiencies, respectively, than cFΦR<sub>4</sub>.

We next applied the reversible bicyclization strategy to generate a cell-permeable, biologically active peptidyl inhibitor against the NEMO-IKK interaction. Despite of its *in vivo* efficacy, the linear Antp-NBD peptide has poor pharmacokinetics, due to rapid proteolytic degradation in serum ( $t_{1/2} \sim 15$  min).<sup>[10]</sup> We envisioned that conversion of Antp-NBD into a conformationally constrained bicyclic structure would substantially increase its proteolytic stability. The CPP motif RRRRΦF was fused to the N-terminus of NBD, TALDWSWLQT, and the N- and C-terminal threonine residues were replaced with two cysteines (Table 1, peptide **4**, Figure S2 for detailed structure). The peptide fusion was bicyclized around the BMB scaffold via two disulfide bonds as described above, to give bicyclic peptide **4** as the predominant product (Figure S3A). As a control, we also prepared peptide **5** (Figure S2 for detailed structure), which is structurally similar to peptide **4** but contains two Ala residues in place of the two Trp residues. It was previously shown that replacement of the Trp residues with alanine largely abolished NEMO binding.<sup>[9]</sup>

Peptides **4** and **5** were labeled with FITC at the side chain of a lysine added to their C-termini and their cellular entry was assessed by flow cytometry. Both peptides entered HeLa

cells efficiently, exhibiting MFI values that were 3- and 2-fold higher than that of cF $\Phi$ R<sub>4</sub>, respectively (Figure 1a). The NEMO-binding affinity of peptides **4** and **5** was determined using a homogenous time-resolved fluorescence (HTRF) assay.<sup>[16]</sup> Briefly, in the presence of an anti-glutathione-S-transferase (GST) antibody labeled with a fluorescence donor (Tb) and streptavidin labeled with a fluorescence acceptor (d2), binding of GST-NEMO to a biotinylated IKK $\beta$  fragment (amino acids 701–745)<sup>[17]</sup> results in a resonance energy transfer. Addition of a NEMO inhibitor blocks the NEMO-IKK $\beta$  interaction and reduces the HTRF signal. In the presence of 5 mM tris(carboxylethyl)phosphine (TCEP), which is expected to completely reduce the disulfide bonds in peptides **4** and **5**, peptide **4** inhibited the NEMO-IKK $\beta$  interaction in a concentration-dependent manner, with a half-maximal inhibitory concentration (IC<sub>50</sub>) value of  $3.5 \pm 0.2 \mu\text{M}$  (Figure 1b). Under the same conditions, Antp-NBD showed an IC<sub>50</sub> value of  $\sim 50 \mu\text{M}$ , in agreement with the previously reported binding affinity.<sup>[16]</sup> As expected, up to 100  $\mu\text{M}$  peptide **5** caused only minor inhibition of the interaction. Since substitution of the two cysteine residues for threonine did not significantly change the NEMO binding affinity (Figure S4), the enhanced NEMO binding of peptide **4** relative to Antp-NBD is likely caused by additional interactions between the phenylalanine of the CPP motif (RRRR $\Phi$ F) and the NEMO protein surface. IKK $\beta$  contains a phenylalanine at the same position (Phe-734). The crystal structure of the NEMO-IKK $\beta$  complex shows that the side chain of Phe-734 inserts into a hydrophobic pocket on the NEMO surface.<sup>[16]</sup> Thus, the phenylalanine in peptide **4** likely plays dual roles of cellular entry and NEMO binding.

The ability of the bicyclic peptides to modulate the NEMO-IKK interaction inside the cell was assessed by monitoring the TNF $\alpha$ -induced activation of NF- $\kappa$ B. HEK293 cells transfected with a luciferase reporter gene under the control of NF- $\kappa$ B were first treated with varying concentrations of a peptide for 1 h and then TNF $\alpha$ .<sup>[9,10e]</sup> In the absence of any inhibitory peptide, treatment with 5 ng/mL TNF $\alpha$  increased the luciferase activity from a basal level of 177 arbitrary units (AU) to 715 AU (data not shown). Peptide **4** reduced the TNF $\alpha$ -induced luciferase activity in a dose-dependent manner, with an IC<sub>50</sub> value of  $\sim 20 \mu\text{M}$  (Figure 1c). In contrast, the control peptide **5** had no significant effect on NF- $\kappa$ B signaling at 20  $\mu\text{M}$  and resulted in  $\sim 10\%$  inhibition at the highest concentration tested (40  $\mu\text{M}$ ). Consistent with the earlier report,<sup>[9]</sup> Antp-NBD (peptide **1**) also caused concentration-dependent inhibition, but showed an IC<sub>50</sub> value of 140  $\mu\text{M}$ . The higher potency of bicyclic peptide **4** relative to Antp-NBD in the cellular assay is likely the results of both improved cellular entry efficiency (Figure 1a) and greater NEMO-binding affinity (Figure 1b). In vitro treatment of bicyclic peptide **4** with 5 mM glutathione for 2 h completely reduced the disulfide bonds (Figure S3b), suggesting that peptides **2–5** should undergo complete reduction upon cytosolic entry.

Finally, the proteolytic stability of peptide **4** and Antp-NBD was tested by incubating the peptides in human serum for varying lengths of time and the remaining amounts of intact peptides were quantitated by analytical HPLC. For comparison, we synthesized a control peptide (Table 1, peptide **6**), which has the same sequence as peptide **4** but only its CPP motif was cyclized. Peptide **6** also reduced the TNF $\alpha$ -induced luciferase activity in a dose-dependent manner, with an IC<sub>50</sub> value of  $\sim 40 \mu\text{M}$  (Figure S5). In agreement with the

previous reports,<sup>[10]</sup> Antp-NBD was rapidly degraded by human serum, with a half-life of ~15 min (Figure 1d). In contrast, bicyclic peptide **4** showed a half-life of ~10 h, and 23% of the peptide remained intact after 20 h of incubation at 37 °C. The monocyclic control peptide **6** was also rapidly degraded (with a half-life of ~30 min), likely due to proteolysis of the linear NBD sequence. We had previously shown that linear peptidyl cargos attached to the Gln side chain of cF $\Phi$ R<sub>4</sub> were rapidly degraded in human serum.<sup>[15]</sup>

In conclusion, a simple method has been developed to efficiently deliver peptidyl ligands into mammalian cells, by fusing the peptide with a short CPP motif and reversibly cyclizing the fusion peptide through disulfide bonds. The resulting bicyclic peptide has greatly enhanced cellular uptake as well as proteolytic stability. This strategy should be applicable to delivering any linear peptides.

## Supplementary Material

Refer to Web version on PubMed Central for supplementary material.

## Acknowledgments

Financial support from the National Institutes of Health (GM110208) is gratefully acknowledged. We thank Dr. M. Pellegrini for the IKK $\beta$ (701–745) plasmid and W. Lian and J. S. Stewart for technical assistance.

## References

1. For excellent reviews on protein-protein interactions, see: Wells J, McClendon C. *Nature*. 2007; 450:1001. [PubMed: 18075579] Nevola L, Giralt E. *Chem Commun*. 2015; 51:3302–15. Pelay-Gilmeno M, Glas A, Koch O, Grossmann TN. *Angew Chem Int Ed*. 2015; 54:8896. *Angew Chem*. 2015; 127:9022.
2. For reviews on peptide therapeutics, see: Craik DJ, Fairlie DP, Liras S, Price D. *Chem Biol Drug Des*. 2013; 81:136. [PubMed: 23253135] Fosgerau K, Hoffmann T. *Drug Disc Today*. 2015; 20:122.
3. Rezai T, Bock JE, Zhou MV, Kalyanaraman C, Lokey RS, Jacobson MP. *J Am Chem Soc*. 2006; 128:14073. [PubMed: 17061890]
4. For selected examples on peptide N-methylation, see: Chatterjee J, Gilon C, Hoffman A, Kessler H. *Acc Chem Res*. 2008; 41:1331. [PubMed: 18636716] White TR, Renzelman CM, Rand AC, Rezai T, McEwen CM, Gelev VM, Turner RA, Linington RG, Leung SSF, Kalgutkar AS, Bauman JN, Zhang YZ, Liras S, Price DA, Mathiowetz AM, Jacobson MP, Lokey RS. *Nat Chem Biol*. 2011; 7:810. [PubMed: 21946276]
5. Oeckinghaus A, Ghosh S. *Cold Spring Harb Perspect Biol*. 2009; 1:a000034. [PubMed: 20066092]
6. a) Baud V, Karin M. *Nat Rev Drug Discov*. 2009; 8:33. [PubMed: 19116625] b) Sun S-C, Chang J-H, Jin J. *Trends Immunol*. 2013; 34:282. [PubMed: 23434408] c) Herrington FD, Carmody RJ, Goodyear CS. *J Biomol Screen*. 2016; 21:223. [PubMed: 26597958] d) Cildir G, Low KC, Tergaonkar V. *Trends Mol Med*. 2016; 22:414. [PubMed: 27068135]
7. a) Yamaoka S, Courtois G, Bessia C, Whiteside ST, Weil R, Agou F, Kirk HE, Kay RJ, Israel A. *Cell*. 1998; 26:1231. b) Rothwarf DM, Zandi E, Natoli G, Karin M. *Nature*. 1998; 395:297. [PubMed: 9751060]
8. a) Gupta SC, Sundaram C, Reuter S, Aggarwal BB. *Biochim Biophys Acta*. 2011; 1799:775. b) Herndon TM, Deisseroth A, Kaminskas E, Kane RC, Koti KM, Rothmann MD, Habtemariam B, Bullock J, Bray JD, Hawes J, Palmby TR, Jee J, Adams W, Mahayni H, Brown J, Dorantes A, Sridhara R, Farrell AT, Pazdur R. *Clin Cancer Res*. 2013; 19:4559. [PubMed: 23775332]
9. May MJ, D'Acquisto F, Madge LA, Glockner J, Poerber JS, Ghosh S. *Science*. 2000; 289:1550. [PubMed: 10968790]

10. a) Jimi E, Aoki K, Saito H, D'Acquisto F, May MJ, Nakamura I, Sudo T, Kojima T, Okamoto F, Fukushima H, Okabe K, Ohya K, Ghosh S. *Nat Med*. 2004; 10:617. [PubMed: 15156202] b) Dai S, Hirayama T, Abbas S, Abu-Amer Y. *J Biol Chem*. 2004; 279:37219. [PubMed: 15252035] c) Shibata W, Maeda S, Hikiba Y, Yanai A, Ohmae T, Sakamoto K, Nakagawa H, Ogura K, Omata M. *J Immunol*. 2007; 179:2681. [PubMed: 17709478] d) Dave SH, Tilstra JS, Matsuoka K, Li F, Karrasch T, Uno JK, Sepulveda AR, Jobin C, Baldwin AS, Robbins PD, Plevy SE. *J Immunol*. 2007; 179:7852. [PubMed: 18025231] e) Gaurier-Hausser A, Patel R, Baldwin AS, May MJ, Mason NJ. *Clin Cancer Res*. 2011; 17:4661. [PubMed: 21610150] f) Peterson JM, Kline W, Canan BD, Ricca DJ, Kaspar B, Delfin DA, DiRienzo K, Clemens PR, Robbins PD, Baldwin AS, Food P, Kaumaya P, Freitas M, Kornegay JN, Mendell JR, Rafael-Fortney JA, Guttridge DC, Janssen PM. *Mol Med*. 2011; 17:508. [PubMed: 21267511] g) Delfin DA, Xu Y, Peterson JM, Guttridge DC, Rafael-Fortney JA, Janssen PM. *J Transl Med*. 2011; 9:68. [PubMed: 21586145] h) Reay DP, Yang M, Watchko JF, Daood M, O'Day TL, Rehman KK, Guttridge DC, Robbins PD, Clemens PR. *Neurobiol Dis*. 2011; 43:598. [PubMed: 21624467] i) Kornegay JN, Peterson JM, Bogan DJ, Kline W, Bogan JR, Dow JL, Fan Z, Wang J, Ahn M, Zhu H, Styner M, Guttridge DC. *Skelet Muscle*. 2014; 4:18. [PubMed: 25789154] j) Habineza Ndikuyeze G, Gaunier-Hausser A, Patel R, Baldwin AS, May MJ, Food P, Krick E, Probert KJ, Masson NJ. *PLoS One*. 2014; 9:e95404. [PubMed: 24798348]
11. a) Qian Z, Liu T, Liu YY, Briesewitz R, Barrios AM, Jhiang SM, Pei D. *ACS Chem Biol*. 2013; 8:423. [PubMed: 23130658] b) Qian Z, LaRochelle JR, Jiang B, Lian W, Hard RL, Selner NG, Luechapanichkul R, Barrios AM, Pei D. *Biochemistry*. 2014; 53:4034. [PubMed: 24896852]
12. Qian Z, Martyna A, Hard RL, Wang J, Appiah-Kubi G, Coss C, Phelps MA, Rossman JS, Pei D. *Biochemistry*. 2016; 55:2601. [PubMed: 27089101]
13. Upadhyaya P, Qian Z, Selner NG, Clippinger SR, Wu Z, Briesewitz R, Pei D. *Angew Chem, Int Ed*. 2015; 54:7602. *Angew Chem*. 2015; 127:7712.
14. Trinh TB, Upadhyaya P, Qian Z, Pei D. *ACS Comb Sci*. 2016; 18:75. [PubMed: 26645887]
15. Qian Z, Xu X, Amacher JF, Madden DR, Cormet-Boyaka E, Pei D. *Angew Chem Int Ed*. 2015; 54:5874. *Angew Chem*. 2015; 127:5972.
16. a) Rushe M, Silvian L, Bixler S, Chen LL, Cheung A, Bowes S, Cuervo H, Berkowitz S, Zheng T, Guckian K, Pellegrini M, Lugovskoy A. *Structure*. 2008; 16:798. [PubMed: 18462684] b) Gotoh Y, Nagata H, Kase H, Shimonishi M, Ido M. *Anal Biochem*. 2010; 405:19. [PubMed: 20522330]
17. Gao B, Audu CO, Cochran JC, Mierke DF, Pellegrini M. *Biochemistry*. 2014; 53:6776. [PubMed: 25286246]

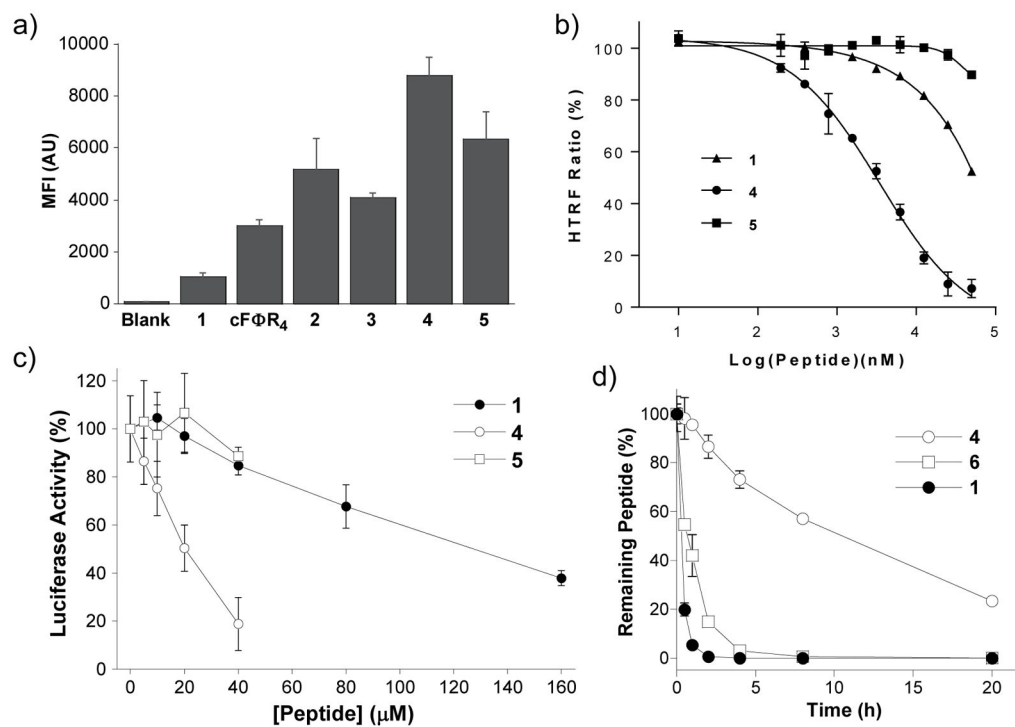
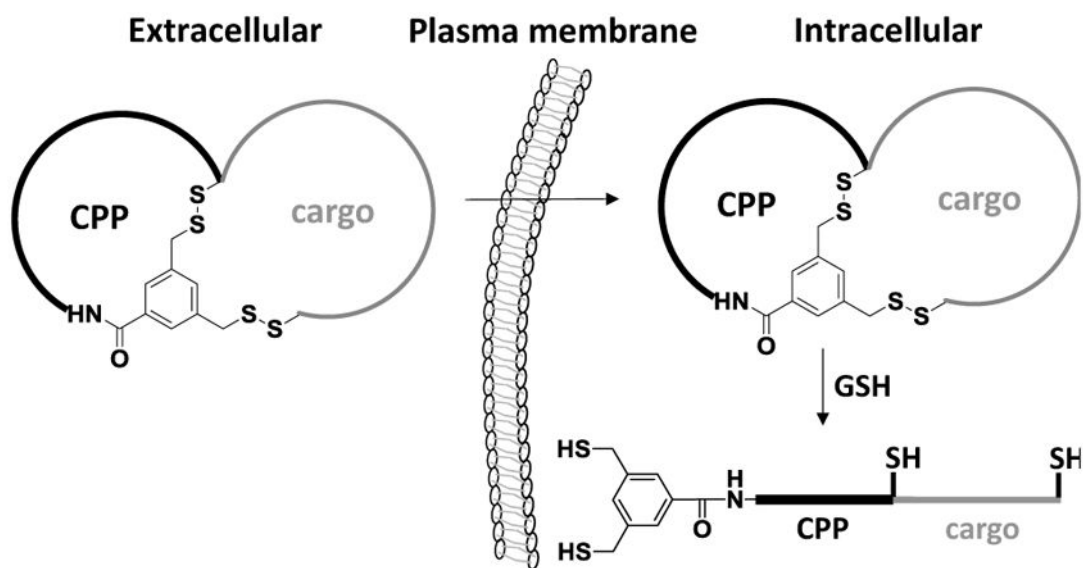


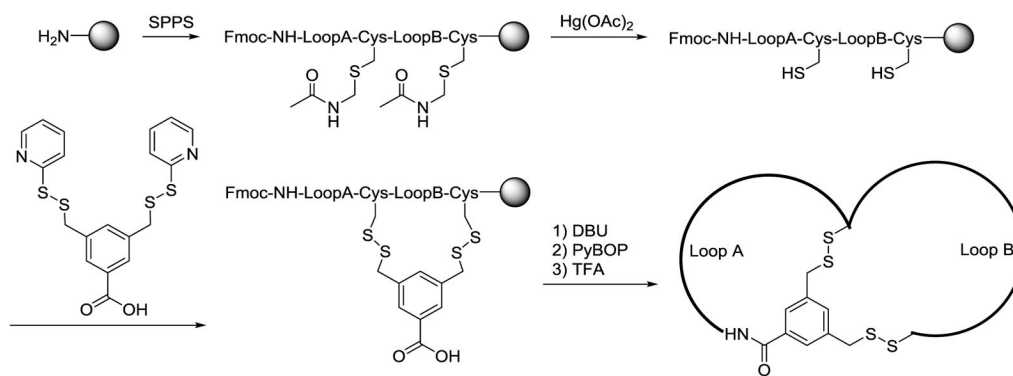
**Figure 1.**

a) MFI of HeLa cells after 2-h treatment with 5 μM FITC-labeled peptide cFΦR<sub>4</sub> or 1–5, as determined by flow cytometry analysis. Blank, no peptide. b) Inhibition of the NEMO-IKKγ interaction by peptides 1, 4, and 5 as monitored by the HTRF assay. c) Dose-dependent inhibition of TNFα induced activation of NF-κB signaling in HEK293 cells by peptides 1, 4, and 5. d) Comparison of the serum stability of peptides 1, 4, and 6. Data reported are the mean ± SD of three independent experiments.



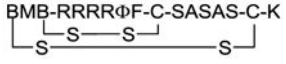
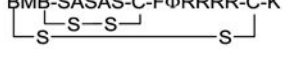
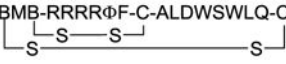
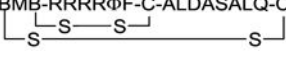
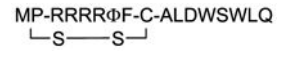


**Scheme 1.**  
A reversible peptide bicyclization strategy. GSH, glutathione.



**Scheme 2.**  
Solid-phase synthesis of disulfide-mediated bicyclic peptides.

**Table 1**Sequences of peptides in this work<sup>[a]</sup>

Peptide ID	Sequence
1	RQIKIWFQNRRMKWKKGG-TALDSWLQTE
2	BMB-RRRRΦF-C-SASAS-C-K 
3	BMB-SASAS-C-FΦRRRR-C-K 
4	BMB-RRRRΦF-C-ALDWSWLQ-C 
5	BMB-RRRRΦF-C-ALDASALQ-C 
6	MP-RRRRΦF-C-ALDWSWLQ 

<sup>[a]</sup>BMB, 3,5-bis(mercaptomethyl)benzoyl; Φ, L-2-naphthylalanine; MP, 3-mercaptopropionyl. See Figure S1 for detailed structures.